

WFPC2 Dark Current vs. Time

J. Mack, J. Biretta, S. Baggett, C. Proffitt
June 7, 2001

ABSTRACT

On-going measurements of the dark current in the WFPC2 detectors indicate that the average level of dark current has been slowly increasing over the instrument's lifetime. We have analyzed more recent dark current data, now covering the period from September 1994 to January 2001. This analysis shows that after late-1998, the dark current is increasing more slowly than expected and could possibly be leveling off temporarily. The STIS CCD dark current shows a similar effect. This behavior may be linked to the solar cycle, where the cosmic ray rate is reduced at solar maximum, causing the median dark current to be lower. If this hypothesis is correct, we expect the dark current to eventually continue increasing at its previous rate.

Introduction

The last detailed study of the WFPC2 dark current and its variation with time is described in WFPC2 TIR 98-03. This report, written at the end of 1998, indicates that the average dark current level is increasing approximately linearly with time and will most likely continue to do so at a fixed rate. To follow up on these predictions, we have examined weekly dark images for dates including the previous analysis up to the present day (1994-2001).

Data & Analysis

The specific dark images chosen for this study were taken just after WFPC2's monthly decontamination. This avoids artificially elevating the measured dark current by eliminating any uncharacterized hot pixels. Each weekly dark image is created from 5 separate WFPC2 dark exposures of 1800 seconds each. These files were combined using the STS-DAS task *mkdark* to generate cosmic-ray cleaned images. The standard *mkdark*

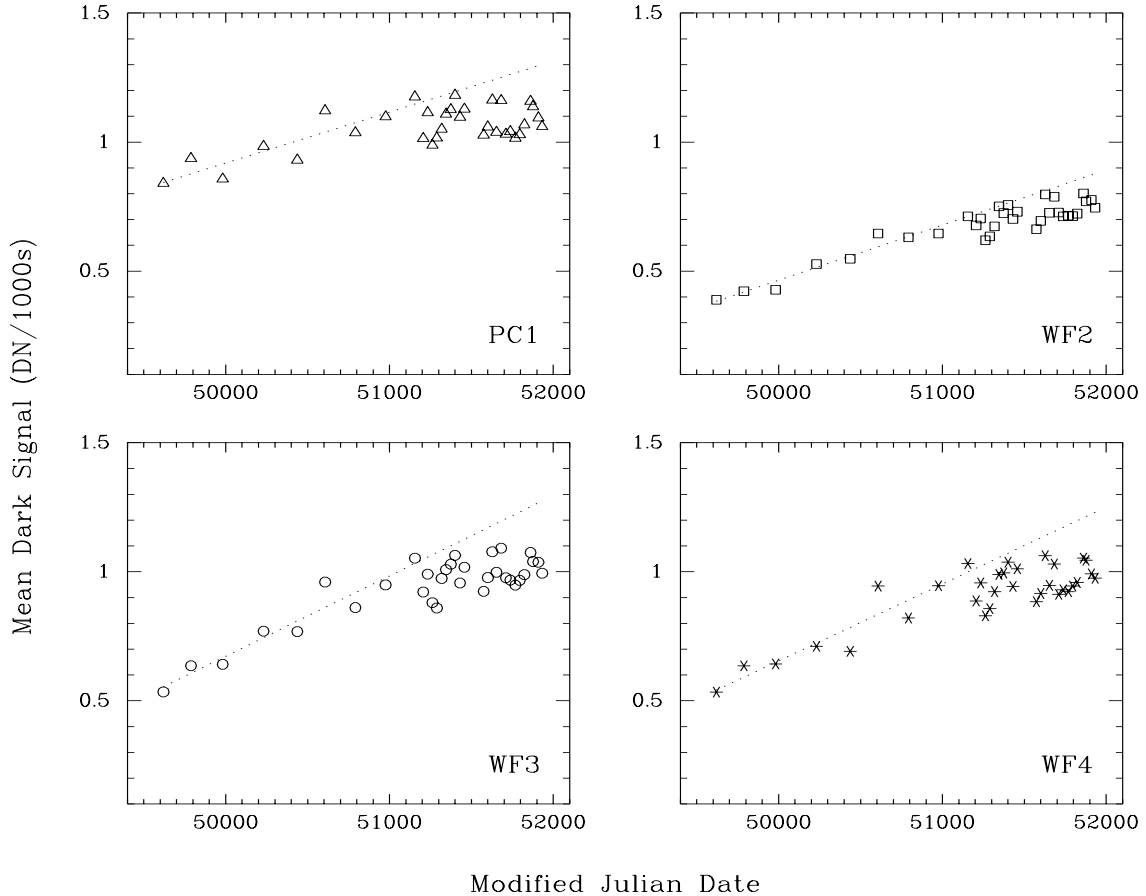
parameters for generating weekly darks were set: $\sigma=4,4,3,2$, $radius=0$, $pfactor=0$, $hot-thresh=4096$, $minval=-99$, $initial=min$, $readnoise=1.73$, $gain=7.5$, and $scalenoise=0$.

The dark current is relatively flat across the central region of each CCD and drops off in strength toward the edges. We thus determined the median dark current value for the central 400x400 pixel region of each chip. Prior to doing statistics, an image mask was created from known hot pixels at the time of observation. These hot pixels were omitted from the dark current measurements. We present a table of the median dark current in each CCD in the Appendix, normalized to units of DN/1000sec.

Figure 1 shows the measured dark levels for the central 400 x 400 pixels of each CCD chip at gain 7. Each data point represents the median of 5 raw 1800s dark frames (after rejection of cosmic rays and bias subtraction, and normalized to units of DN /1000 sec). Over this 6.5 year period, the dark current has increased by a factor of about 2.0 in the WFC CCDs and by a factor of 1.3 in the PC. A small increase in the cold junction temperatures over this time period was observed as well; however, the temperature change accounts for only a very small portion of the increase in dark current.

We note that after December 1998 (e.g. MJD > 51200), the dark current increases more slowly or even begins to level off. The recent dark current values are clearly lower than expected based on a linear extrapolation of the early data points. The line plotted presents this extrapolation for data up to Dec 1998. To further establish the reality of this effect, we analyzed additional darks for epochs after 1998; these monthly points further confirm the effect (Figure 1).

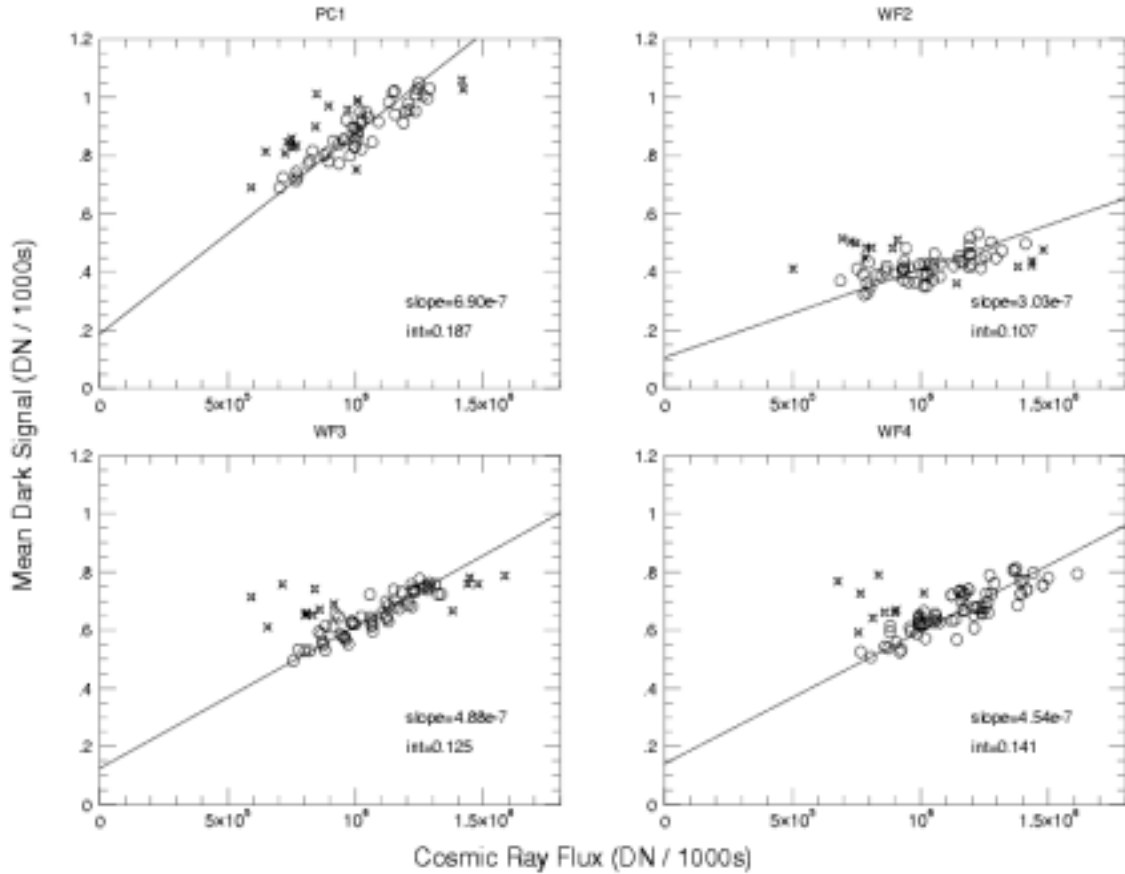
Figure 1: Median Dark Current vs. Date for the PC1, WF2, WF3, and WF4 CCDs. Units are in DN / 1000sec (gain=7 e/DN). The dashed line represents a linear fit to the data through December 1998 (MJD < 51200).



Comparison with Number of Cosmic Ray Events

The dark current is known to consist of two components: one from electronic sources in the CCD, and a second whose strength correlates with cosmic ray flux. (See WFPC2 Instrument Handbook, Chapter 4). The second component is thought to be caused by fluorescence (or scintillation) of the CCD windows. In Figure 2, we present the dark count rate as a function of cosmic ray flux in each window. This plot is taken from Chapter 4 of the WFPC2 Instrument Handbook. The PC1 dark current has the greatest sensitivity to cosmic rays, while the WF2 dark current has the least.

Figure 2: Dark Signal vs. Cosmic Ray Flux for the PC1, WF2, WF3, WF4. Slopes and intercepts are given on the plots. Units are DN/1000s (gain=7 e/DN). This plot was taken from the WFPC2 Instrument Handbook; data plotted are prior to June 1996.



We believe that the recent slowing of the dark current increase may be linked to the solar cycle. After 1998, we are approaching solar maximum which has the effect of reducing the cosmic ray flux at HST's low Earth orbit. In Figure 3, we present the effect of "solar modulation" from the Bartol Research Institute Neutron Monitor Program:

<http://www.bartol.udel.edu/~neutronm/>. Solar modulation refers to the influence the Sun exerts upon the intensity of galactic cosmic rays. As solar activity rises (top panel), the count rate recorded by a neutron monitor in McMurdo Antarctica decreases (bottom panel).

Figure 3: Solar Cycle and Cosmic Ray Counts (Neutrons) vs. Year.

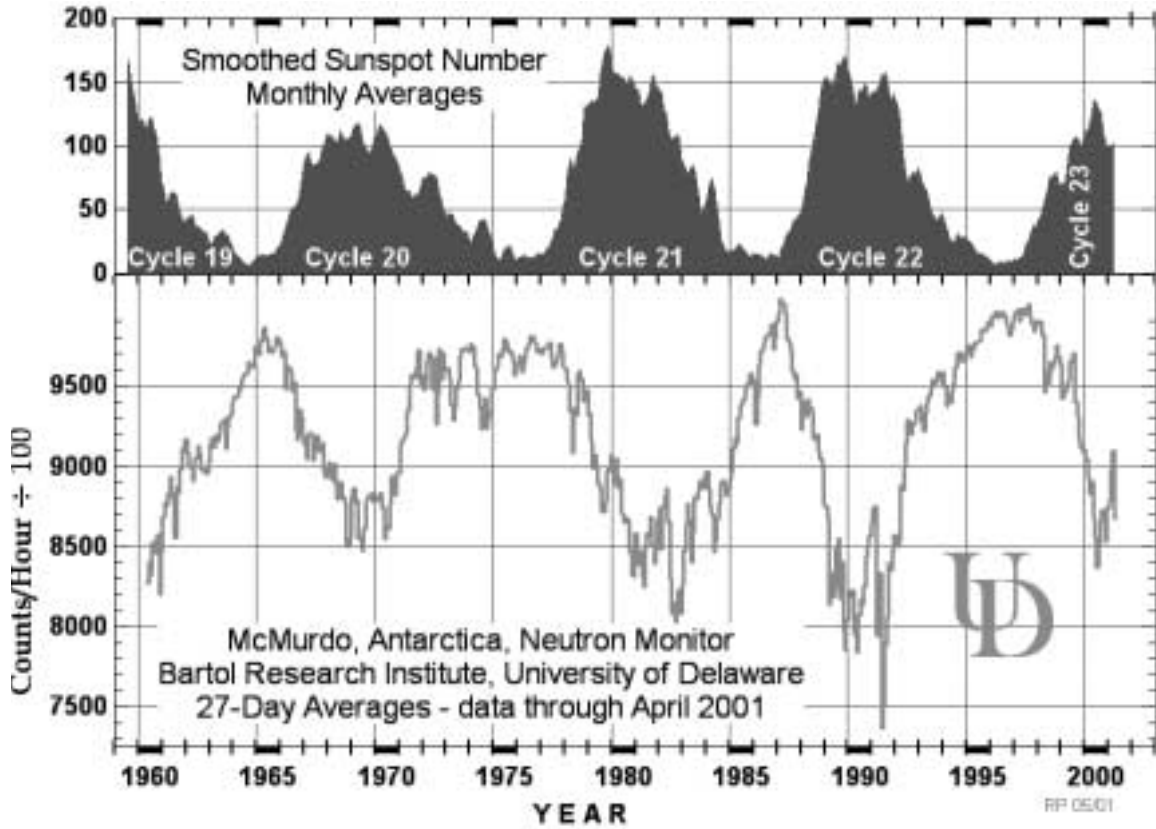
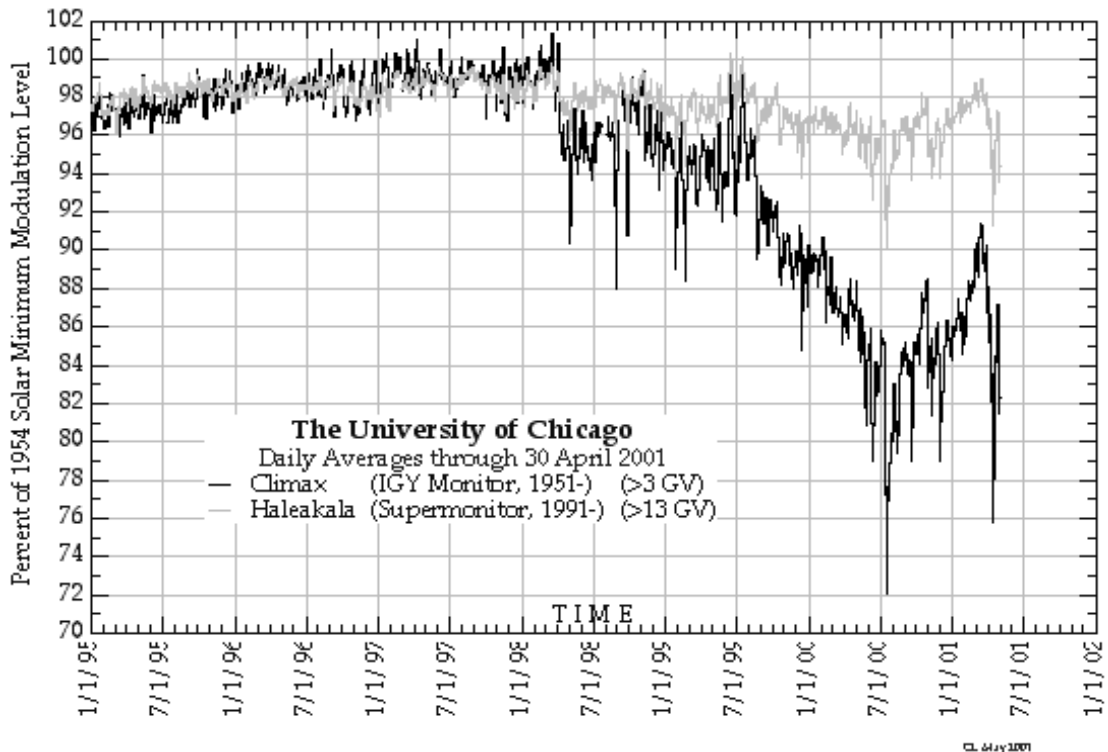


Figure 4: Cosmic Ray Rate (Neutrons) vs. Year.



The decrease in detected cosmic rays for the current solar maximum is shown in greater detail in Figure 4. This plot was taken from the University of Chicago Neutron Monitoring Program website: http://ulysses.uchicago.edu/NeutronMonitor/neutron_mon.html.

Both figures indicate that the solar maximum causes an approximate 20% decrease in the cosmic ray flux. This would lead to a reduction in the “second component” of the WFPC2 dark current caused by cosmic ray induced fluorescence in the CCDs windows. Both the dark current level-off (Figure 1) and the reduction in cosmic rays (Figure 4) begin near the end of 1998, as we would expect if they are directly connected.

Another way to present the dark current data in Figure 1 is to examine the departure of the later data from the linear fit made to the pre-1999 data. This is shown in Figure 5. All CCDs show a similar ~20% departure by early 2001. While this is roughly consistent with the ~20% reduction in cosmic ray flux at solar maximum, it is possible that this quantitative agreement is fortuitous, since the fluorescence effect and the solar cosmic ray modulation may both have (complex) energy dependencies.

Figure 5: Dark Ratio (Fit / Data) vs. Date. The fit includes data through December 1998 (MJD < 51200). The ratio gives the percent difference of the predicted dark current and the measured value.

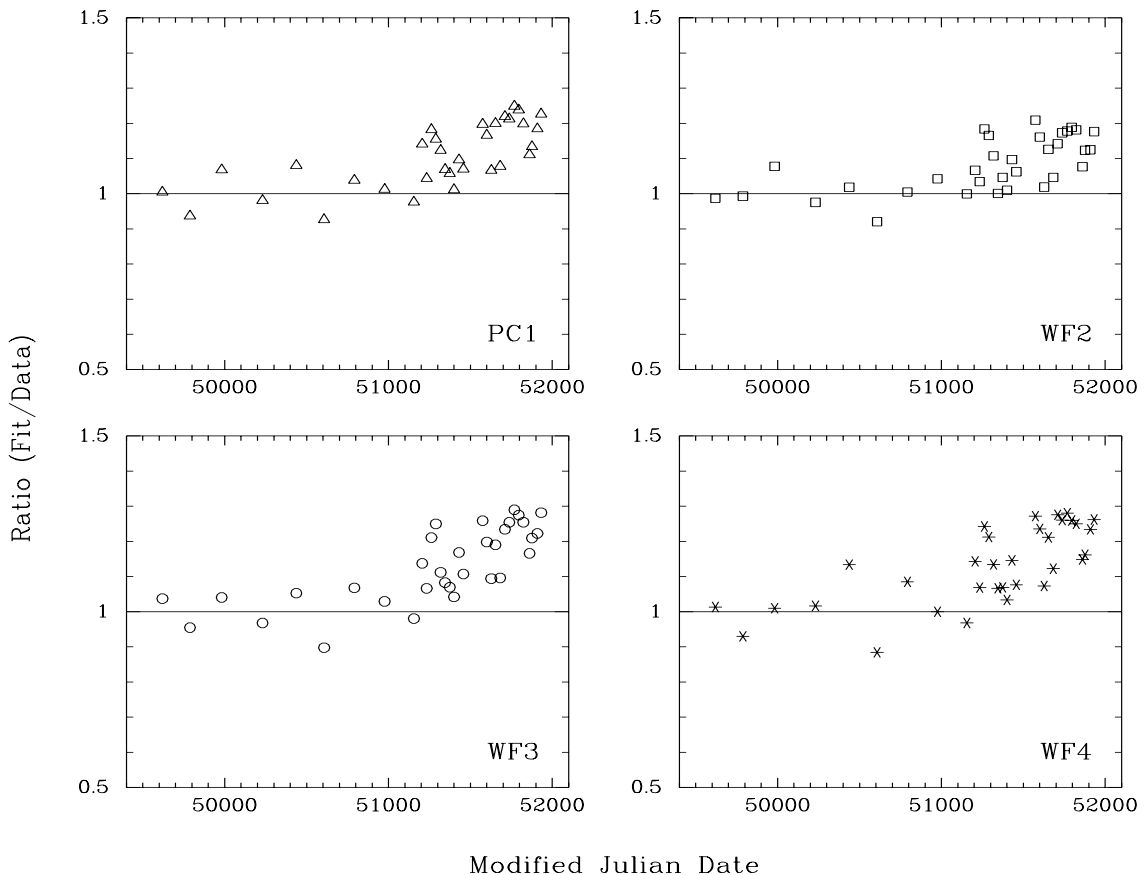
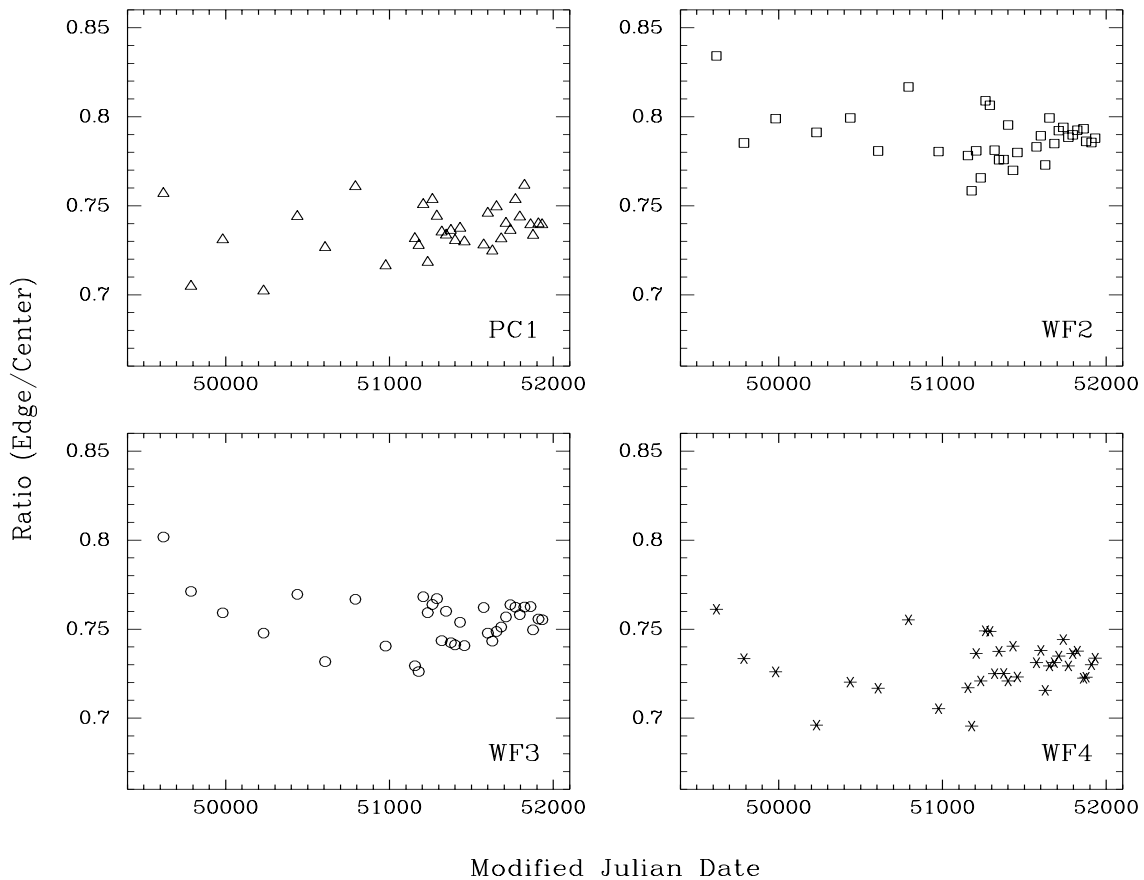


Figure 6: Ratio Edge/Center. The “edge” includes a region 50 pixels wide around the border of each chip. The “center” is a 400x400 pixel region in the center of each chip.



To further study the nature of the observed dark current trend, we make use of the fact that the strength of the dark current drops towards the edges of each CCD. This drop is consistent with luminescence from the CCD windows, shadowed by a field stop mask just in front of the CCD. In other words, the CCD edges see a smaller solid angle of the windows than the CCD centers. We therefore measured the median dark current at the outer edge of each CCD, using a 50 pixel-wide strip. We then compared this value with the dark current at the center of each chip. In Figure 6, we plot the *edge:center* dark current ratio. This ratio shows no significant dependence on the date of observation.

Figure 2 (Dark Current vs. Cosmic Ray Flux) was taken from the WFPC2 Instrument Handbook and includes data taken at early epochs (prior to June 1996). This plot shows that the luminescence of the CCD windows clearly dominates any electronic component. That is, the dark current extrapolates to very low levels at zero cosmic ray flux. The constancy of the *edge:center* ratio (Figure 6) in the presence of the large long-term dark

current increase (Figure 1) indicates : 1.) that fluorescence continues to dominate, and 2.) that the long-term increase in dark current must be primarily due to radiation damage in the CCD windows causing them to generate more light per cosmic ray.

For example, let us instead consider a scenerio in which the fluorescence remained constant and the long-term dark current increase were attributed to electronics in the CCD. Then we might expect the *edge:center* ratios for WF3 and WF4, which exhibit an approximate factor of two long-term dark current increase, to grow from the observed ~ 0.75 value to ~ 0.87 as the fluorescence effect becomes diluted by electronic CCD dark current. Clearly no such increase is seen.

It is possible that *some* of the observed “level-off” is attributable to an electronic dark current component which grows until ~ 1999 and then levels off, but it is clear that fluorescence must greatly dominate any electronic component.

Comparison with Number of Hot Pixels

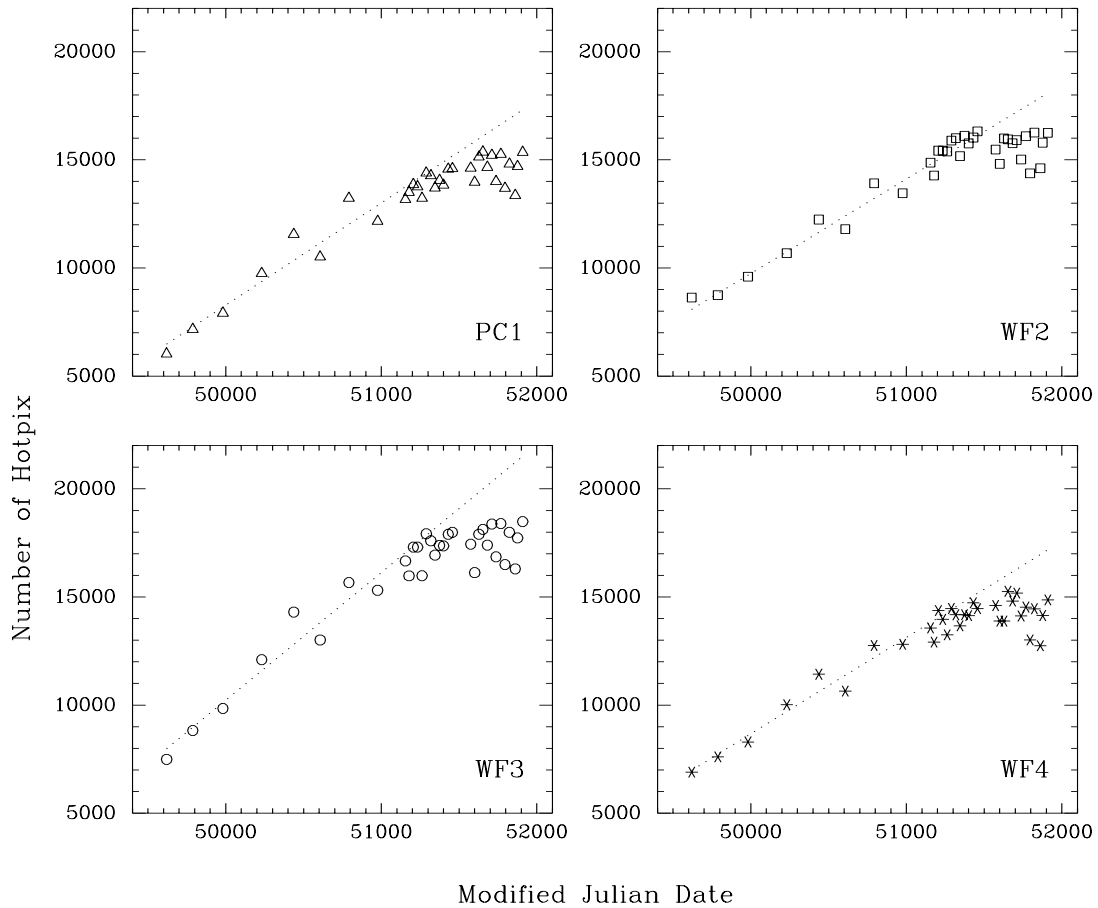
As an additional means of understanding the dark current behavior, we also examined the number of hot pixels detected on each chip. In Figure 7 we plot the number of hot pixels as a function of date for each corresponding dark measurement from Figure 1.

WFPC2 hot pixel lists are created once per month using weekly darks taken during the month-long period between decontaminations. Pixels are included in this list if they satisfy any *one* of the following criteria:

Maximum current	>	(chip avg) + 5 * (chip rms)
Average dark current	>	(chip avg) + 4 * (chip rms)
Rms variation	>	3 * (chip rms)
Peak-to-peak variation	>	4 * (chip rms)

In Figure 7, we see the same effect as with the median dark current rate: an approximately linear increase with time which begins to level off at the end of 1998. Included in this plot is a fit to the “early” data points, indicating the predicted number of hot pixels. These hot pixels are mostly caused by radiation damage to the CCDs, again as a result of cosmic rays. This effect can also be linked to the solar cycle, where at solar maximum fewer pixels are being damaged by energetic particles. If this hypothesis is correct, we expect that the number of hot pixels will again begin to increase at the old rates, once solar maximum is passed.

Figure 7: Number of Hot Pixels vs. Date. The fit includes data through December 1998 (MJD < 51200).



STIS Dark Current & Hot Pixels

To establish the reality of the apparent trend in the WFPC2 data, we also examined measurements of the dark current in the STIS CCDs. Much of this work was done using the IRAF task *anneal_darks* in the *teststis* package. This task, written by Jeffrey Hayes in October 1998, generates statistics on STIS CCD anneal darks. Ongoing analysis is currently carried out by Charles Proffitt and James Davies. The following description outlines the procedures in the *anneal_darks* task. For more information, refer to STIS ISR 98-06-Rev A.

The raw dark images are run through *calstis* with the following calibration keywords set to perform: DQICORR, BLEVCORR, EXPCORR, CRCORR, BIASCORR. A superdark is then created from data just before an anneal, and a similar superdark is created from data

just after the anneal. Both superdarks are normalized to units of electrons/sec and the median value and other statistics are recorded.

The program then creates an image containing only hot pixels (defined as > 5 sigma of the baseline dark current). The lower threshold for the hot pixel cutoff is measured at several levels: 0.1 e/s, 1.0 e/s, 3.0 e/s, 5.0 e/s, and 10.0 e/s. A comparison is then made of which pixel locations anneal out, which persist, and which are not affected by the anneal. The task generates tables including the number of hot pixels, their brightness, and their location before and after the anneal. Additionally, the change in brightness of each pixel is written to a separate file, along with the pixel locations which do not anneal away.

Using the tables generated by the STIS Instrument Team, we plot the median post-anneal dark count rate (electrons/sec) in Figure 8. We notice in this figure a similar leveling-off behavior in the dark current. This deviation from the linear fit occurs around May 2000, just over a year after we see the effect in the WFPC2 CCDs. This difference in the onset date could well be attributed to differences in the instruments. For example, different components might be affected by cosmic rays of different energies, which are impacted differently by the solar cycle.

In Figure 9, we plot the number of hot pixels measured in the STIS CCDs at four threshold levels: 0.1 e/s, 1.0 e/s, 3.0 e/s, and 10 e/s. The highest energy hot pixels (>10 e/s) appear to increase at approximately a constant rate. The lower energy pixels (0.1 e/s and 1.0 e/s), however, appear to deviate from the expected trend in a manner similar to the median dark current. The linear fit plotted is based on the pre-May 2000 data. This effect is mirrored in the cosmic ray rate shown in Figure 4: the high energy cosmic rays (>13 GV, grey line) only decrease by a few percent from solar minimum to solar maximum, while the lower energy cosmic rays (>3 GV, black line) decrease by $\sim 20\%$. The STIS results generally appear to confirm the WFPC2 results and further confirm an external cause, namely a modulation of the cosmic ray flux by the solar cycle.

However, it is also possible that the STIS dark current level-off is due to some other effect (e.g. instrument aging). While there is a clear connection between cosmic ray flux and luminescence of the WFPC2 CCD windows (Figure 2), no such direct connection is known for STIS. If the predicted upturn in dark current occurs in both instruments once solar maximum is passed, this would confirm the solar modulation hypothesis for STIS.

Figure 8: STIS Dark Signal (electrons/sec) vs. Date. The fit includes data through May 2000 (MJD < 51700).

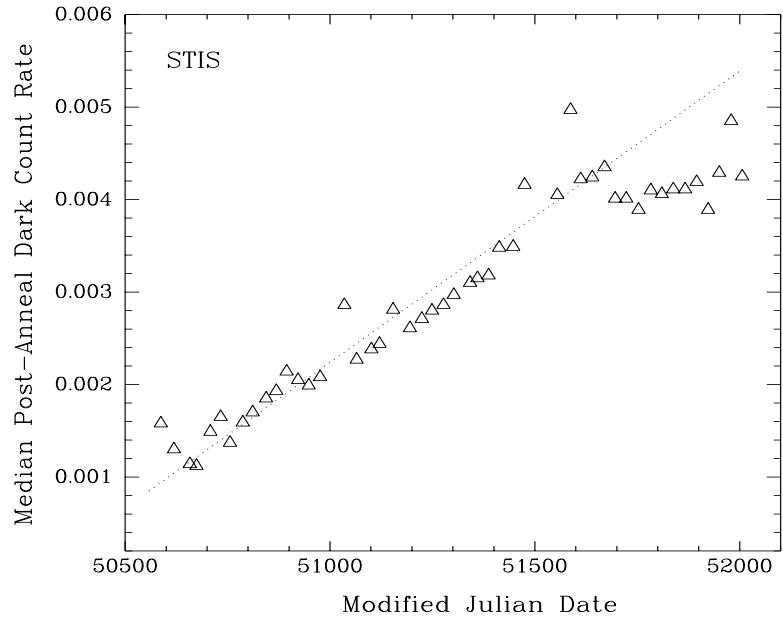
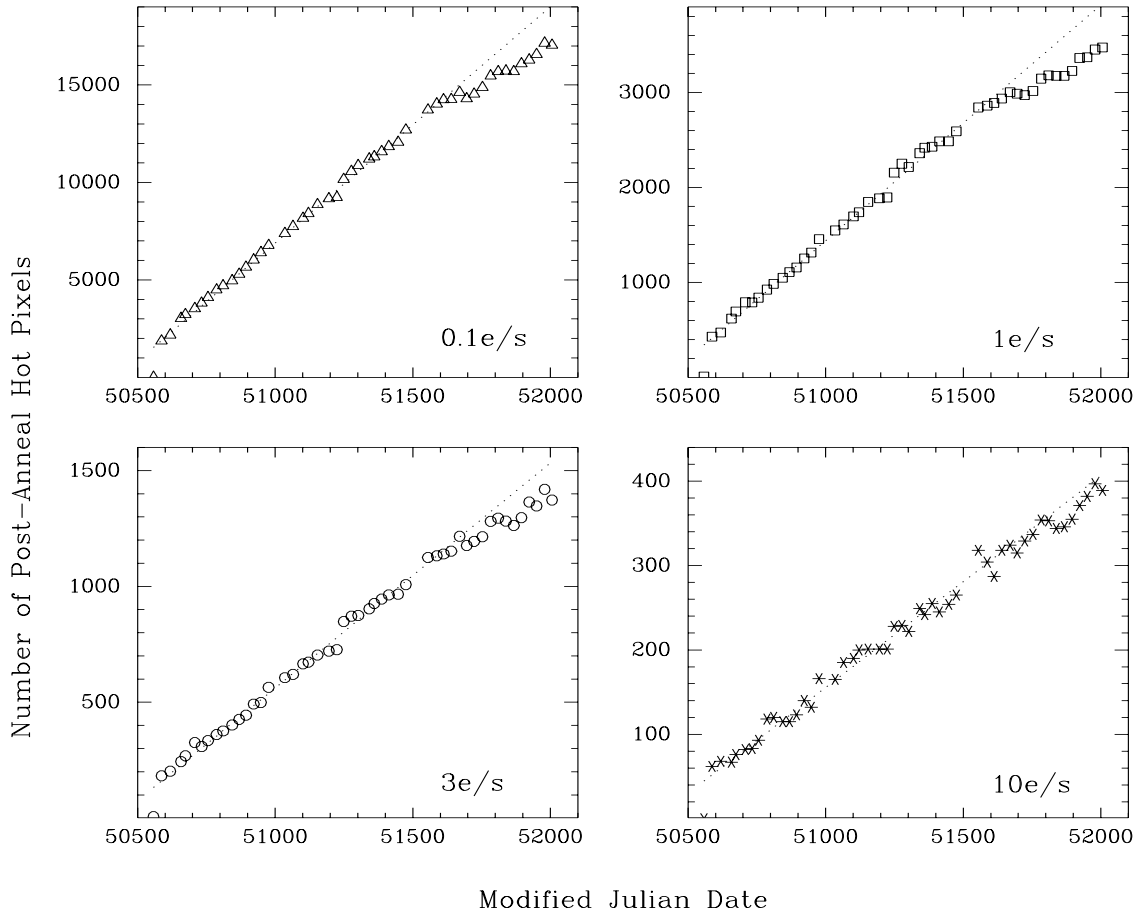


Figure 9: Number of Hot Pixels vs. Date for STIS CCDs.



Conclusions

We have analyzed recent WFPC2 dark current measurements, now covering the period from Sept 1994 to Jan 2001. This analysis shows that after late-1998, the dark current is increasing more slowly than expected. A comparison with the STIS CCD dark current shows a similar effect. We believe these effects are related to the cosmic ray decrease which accompanies the current solar maximum. In particular, the leveling-off of the WFPC2 dark current is probably a direct result of reduced fluorescence by the CCD windows. There is also a leveling-off in the hot pixel creation rate, again attributable to the reduction in cosmic rays. If this hypothesis is correct, we expect the dark current will eventually resume the pre-1998 rate of increase.

Acknowledgements

We would like to thank Charles Proffitt and James Davies for measurements of the STIS dark current and for comments on this ISR. We also acknowledge the University of Chicago neutron monitor operations and research activities, supported by the National Science Foundation Grant ATM-9912341, and the Bartol Research Institute neutron monitor program, supported by the National Science Foundation Grant ATM-0000315.

References

WFPC2 Technical Instrument Report 98-03: "WFPC2 Dark Current Evolution". S. Baggett, S. Casertano, M.S. Wiggs.

STIS Instrument Science Report 98-06-Rev A: "STIS CCD Anneals". J. Hayes, J. Christensen, P. Goudfrooij.

Appendix

Median dark current levels, in DN / 1000sec, for the central 400x400 pixel region of each WFPC2 chip. (gain=7 e/DN)

Date	MJD	PC1	WF2	WF3	WF4
09/25/94	49620	0.84	0.39	0.53	0.53
03/12/95	49788	0.94	0.42	0.64	0.64
09/22/95	49982	0.86	0.43	0.64	0.64
05/28/96	50231	0.98	0.53	0.77	0.71
12/20/96	50437	0.93	0.55	0.77	0.69
06/08/97	50607	1.12	0.65	0.96	0.94

Instrument Science Report WFPC2 2001-05

Date	MJD	PC1	WF2	WF3	WF4
12/10/97	50792	1.04	0.63	0.86	0.82
06/12/98	50976	1.10	0.65	0.95	0.95
12/08/98	51155	1.18	0.71	1.05	1.03
01/28/99	51206	1.01	0.68	0.92	0.89
02/24/99	51233	1.11	0.70	0.99	0.96
03/25/99	51262	0.99	0.62	0.88	0.83
04/21/99	51289	1.02	0.63	0.86	0.86
05/20/99	51318	1.05	0.67	0.97	0.92
06/16/99	51345	1.11	0.75	1.01	0.99
07/15/99	51374	1.13	0.72	1.03	1.00
08/10/99	51400	1.18	0.76	1.06	1.04
09/09/99	51430	1.10	0.70	0.96	0.94
10/06/99	51457	1.13	0.73	1.02	1.01
01/31/00	51574	1.03	0.66	0.92	0.88
02/26/00	51600	1.06	0.69	0.98	0.92
03/24/00	51627	1.16	0.80	1.08	1.06
04/19/00	51653	1.04	0.73	1.00	0.95
05/18/00	51682	1.16	0.79	1.09	1.03
06/15/00	51710	1.03	0.73	0.98	0.91
07/12/00	51737	1.04	0.71	0.97	0.93
08/12/00	51768	1.02	0.72	0.95	0.92
09/08/00	51795	1.03	0.71	0.97	0.94
10/06/00	51823	1.07	0.72	0.99	0.96
11/13/00	51861	1.16	0.80	1.07	1.05
11/28/00	51876	1.14	0.77	1.04	1.04
12/31/00	51909	1.09	0.78	1.04	0.99
01/23/01	51932	1.06	0.75	0.99	0.97